Check for updates

Comparative Analysis of Corpus Callosum Lipidome and Transcriptome in Schizophrenia and Healthy Brain

Сравнительный анализ липидома и транскриптома мозолистого тела головного мозга при шизофрении и в здоровом состоянии

doi: 10.17816/CP15491

Original research

Maria Osetrova[1], Olga Efimova[1], Marina Zavolskova[1], Elena Stekolschikova[1], Gleb Vladimirov[1], Dmitry Senko[1], Tatiana Zhuravleva[2], Anna Morozova[3,4], Yana Zorkina[3,4], Denis Andreyuk[3], George Kostyuk[2,3], Evgeniy Nikolaev[1], Philipp Khaitovich[1]

[1] Skolkovo Institute of Science and Technology, Moscow, Russia

[2] Lomonosov Moscow State University, Moscow, Russia

[3] Mental-health clinic No. 1 named after N.A. Alexeev, Moscow, Russia

[4] V. Serbsky National Medical Research Centre of Psychiatry and Narcology of the Ministry of Health of the Russian Federation, Moscow, Russia

Мария Осетрова[1], Ольга Ефимова[1], Марина Завольскова[1], Елена Стекольщикова[1], Глеб Владимиров[1], Дмитрий Сенько[1], Татьяна Журавлева[2], Анна Морозова[3,4], Яна Зоркина[3,4], Денис Андреюк[3], Георгий Костюк[2,3], Евгений Николаев[1], Филипп Хайтович[1]

[1] АНОО ВО «Сколковский институт науки и технологий», Москва, Россия

[2] ФГБОУ ВО «Московский государственный университет имени М.В. Ломоносова», Москва, Россия

[3] ГБУЗ «Психиатрическая клиническая больница № 1 им. Н.А. Алексеева Департамента здравоохранения города Москвы», Москва, Россия

[4] ФГБУ «Национальный медицинский исследовательский центр психиатрии и наркологии им. В.П. Сербского» Минздрава России, Москва, Россия

ABSTRACT

BACKGROUND: Functional and structural studies of the brain highlight the importance of white matter alterations in schizophrenia. However, molecular studies of the alterations associated with the disease remain insufficient.

AIM: To study the lipidome and transcriptome composition of the corpus callosum in schizophrenia, including analyzing a larger number of biochemical lipid compounds and their spatial distribution in brain sections, and corpus callosum transcriptome data. To integrate the results of molecular approaches to create a comprehensive molecular perspective of the disease.

METHODS: A total of 8 brain tissue samples (4 from healthy controls (HC) + 4 from schizophrenia patients (SZ)) were analyzed using high-performance liquid chromatography with mass spectrometry (HPLC-MS) and RNA sequencing for transcriptome profiling. Additionally, 6 brain tissue samples (3 HC + 3 SZ) were analyzed using matrix-assisted laser desorption/ionization mass spectrometric imaging (MALDI-MSI). This approach enabled the characterization of mRNA and lipids in brain tissue samples, and the spatial distribution of selected lipids within brain sections.

RESULTS: The analysis revealed a general trend of reduced lipid levels in the corpus callosum of schizophrenia patients for lipid classes measured by mass spectrometric methods. Specifically, nine lipid classes detected via HPLC-MS showed significant differences in schizophrenia samples, with seven of them having lower median intensity. The results between

CC BY-NC-ND 4.0 license © Authors, 2025

HPLC-MS and MALDI-MSI were highly concordant. Transcriptome analysis identified 1,202 differentially expressed genes, clustered into four functional modules, one of which was associated with lipid metabolism.

CONCLUSION: We identified a series of lipidome and transcriptome alterations in the corpus callosum of schizophrenia patients that were internally consistent and aligned well with previous findings on white matter lipidome changes in schizophrenia. These results add to the existing scope of molecular alterations associated with schizophrenia, shedding light on the biological processes potentially involved in its pathogenesis.

АННОТАЦИЯ

ВВЕДЕНИЕ: Функциональные и структурные исследования мозга свидетельствуют о важной роли изменений белого вещества при шизофрении. Однако исследований молекулярных изменений в белом веществе, связанных с заболеванием, недостаточно.

ЦЕЛЬ: Изучить липидомный и транскриптомный составы мозолистого тела головного мозга при шизофрении и в норме, включая анализ большего числа биохимических классов липидных соединений и их пространственного распределения в срезах мозга, с помощью данных транскриптома. Объединить результаты различных молекулярных подходов для создания комплексной молекулярной картины заболевания.

МЕТОДЫ: Исследовали 8 образцов мозговой ткани: 4 от здоровой контрольной группы (КГ) + 4 от больных шизофренией (Ш) с использованием высокоэффективной жидкостной хроматографии с масс-спектрометрией (ВЭЖХ-МС) и секвенирования транскриптома. Дополнительно 6 образцов мозговой ткани (3 КГ + 3 Ш) проанализировали с помощью масс-спектрометрической визуализации с использованием матрично-активированной лазерной десорбции/ионизации (МАЛДИ-МС). Это позволило выявить относительное количество мРНК и липидов в образцах мозговой ткани, а также определить пространственное распределение некоторых липидов в срезах мозга.

РЕЗУЛЬТАТЫ: Исследование на основании данных масс-спектрометрических методов выявило общую тенденцию к относительно более низкому количеству липидов в мозолистом теле при шизофрении. Измерение количества липидов в образцах мозговой ткани пациентов с шизофренией с помощью ВЭЖХ-МС показало различия в уровнях липидов всех 9 классов. Кроме того, 7 из них имели относительно более низкую медианную интенсивность. Результаты методов ВЭЖХ-МС и МАЛДИ-МС продемонстрировали высокую степень соответствия. Анализ транскриптома определил 1202 дифференциально экспрессируемых гена. Они составляют 4 функциональных модуля, один из которых связан с метаболизмом липидов.

ЗАКЛЮЧЕНИЕ: Мы обнаружили в мозолистом теле головного мозга пациентов с шизофренией ряд изменений липидома и транскриптома, которые внутренне консистентны, а также хорошо согласуются с предыдущими выводами о липидоме белого вещества при шизофрении и дополняют их. Полученные в исследовании данные указывают на биологические процессы, которые могут претерпевать изменения во время развития патологии, и расширяют знания о существующем спектре молекулярных изменений, связанных с шизофренией.

Keywords: *schizophrenia; lipidomics; transcriptomics; mass spectrometry; corpus callosum*
Ключевые слова: *шизофрения; липидом; транскриптом; масс-спектрометрия; мозолистое тело*

INTRODUCTION

Schizophrenia is a multifactorial, distributed, and prevalent mental disorder that affects millions of people worldwide. It is characterized by a range of symptoms, including delusions, hallucinations, incoherent speech and behavior, and cognitive impairment. Despite extensive research, the causes and molecular basis of schizophrenia remain poorly substantiated. Nonetheless, emerging evidence suggests that alterations in the lipid metabolism at the molecular level might be associated with the disorder [1, 2].

In addition, differences in the transcriptomic profile between a schizophrenia and healthy brain appear to be characteristic of this disease [3] and reflect system-level alterations in the molecular composition of the brain in a pathological state [4, 5].

Lipidome is a complete set of lipids present in a particular cell or tissue. Lipids are essential components of cell membranes and play a critical role in a wide range of physiological processes, including energy storage, signal transduction, and membrane traffick [6]. Recent studies have revealed that alterations occur in several classes of the lipids of the corpus callosum lipidome of a brain suffering from schizophrenia, including phospholipids and sphingolipids [7, 8]. What is more, it is known that abnormalities in the corpus callosum (smaller size, shape variation, and loss of connectivity) are common in people with schizophrenia [4, 5].

While the mechanisms underlying these alterations in lipid metabolism are not yet fully understood, several hypotheses have been proposed [9–11]. One hypothesis suggests that alterations in lipid metabolism may disrupt the integrity of cell membranes, leading to neuronal dysfunction and cognitive impairment [12]. Another hypothesis holds that with schizophrenia, the signaling pathways involved in neurotransmission might be disrupted, leading to abnormal neural activity and the development of schizophrenia [13]. Understanding the alterations in the lipidome that are associated with schizophrenia may provide new insights into the mechanisms underlying this disorder. This may also lead to the development of new diagnostic tools. For example, blood lipidome profiling can be used to identify biomarkers for the early detection and diagnosis of schizophrenia [14]. A widely used method in lipidome studies is high-performance liquid chromatography with mass spectrometry (HPLC-MS). This method allows one to identify a large number of compounds within a single analysis. But during sample preparation, the tissue is homogenized, which results in the loss of unique spatial information. The possibilities afforded by matrix-assisted laser desorption/ionization mass spectrometric imaging (MALDI-MSI) allow one to try to solve this problem. Thus, the HPLC-MS method, paired with MALDI imaging, provides information with reliable signal annotations and a high spatial resolution, making it possible to create a comprehensive picture of the structure of the brain lipidome.

Previous studies investigating the differences in brain transcriptome composition and the expression levels of selected gene groups observed previously in schizophrenia primarily focused on the cortical regions [3, 15, 16], while white matter tracts remain underexplored. Moreover, the number of studies that have simultaneously analyzed the lipidome and transcriptome on the same tissue samples in the context of schizophrenia white matter is very limited [7], with none incorporating spatial information. Taken together, this represents a gap in knowledge as regards the comprehensive study of the white matter lipidome of the brain, particularly with regard to a multi-omics approach.

In this paper, we aimed to study the composition of a schizophrenia-associated corpus callosum lipidome and transcriptome, as well as conduct an analysis of a larger number of biochemical classes of lipid compounds, a spatial analysis of the distribution of these compounds in brain sections supported by an analysis of corpus callosum transcriptome data, and, finally, to integrate the results yielded through different molecular approaches to the analysis in order to create a comprehensive molecular picture of the disease.

METHODS

Tissue samples

Samples were prepared from 14 frozen slices of the human corpus callosum: seven from healthy controls (HC) and seven from schizophrenia patients (SZ). Four samples (HC: two males aged 34 and 62, two females aged 34 and 61; SZ: two males aged 36 and 74, two females aged 57 and 62) from each group were used for the HPLC-MS measurements and RNAseq, and three samples (HC: two males aged 58 and 60, female aged 60; SZ: two males aged 69 and 57, female aged 62) from each group were used for the MALDI-MSI experiment. The demographic data of postmortem brain tissue donors and the ribonucleic acid (RNA) integrity number (RIN)[1] of the samples are presented in Table S1 in the Supplementary.

The postmortem human brain samples were provided by the biobank of the Contract Research Organization (CRO)

[1] Ribonucleic acid (RNA) integrity number (RIN) is a measure that evaluates the quality and integrity of RNA in samples; RIN values range from 1 to 10: 10 indicates high-quality, intact RNA; 7–9 suggests good quality with minor damage; 4–6 indicates moderate quality with noticeable degradation; and 1–3 signifies severely degraded RNA that is unsuitable for analysis. RIN allows researchers to ensure that RNA samples are suitable for further experimentation.

National BioService (Saint Petersburg, Russia). No subject in the HC had a history of psychiatric or neurodegenerative disease and no gross anatomical abnormalities were revealed during the pathoanatomical assessment. Brain donors were diagnosed with schizophrenia based on ICD-10 by psychiatrists during inpatient treatment at Mental-health clinic No. 1 named after N.A. Alexeev (Moscow, Russia). Each subject had suffered sudden death with no prolonged agony state. All the post-mortem brain samples were sectioned, placed on aluminum blocks, and frozen on dry ice. All sample transport was conducted on dry ice; and long-term storage, in −80 °C freezers. There was no sample thawing or heating at any point. For mass spectrometric imaging, 300 mg samples were cut using sterile and chilled scalpels, forceps, and tubes. These samples were promptly frozen and stored in a low-temperature freezer at −80 °C until further analysis.

Tissue preparation

Brain samples were sectioned according to The Atlas of the Human Brain [17] by a neuroanatomist using the Leica CM1950 microtome cryostat (Leica Biosystems, China). Cutting was performed at a chamber temperature of −18 °C and sample temperature of −15 °C. The thickness of the sections was set at 20 µm. The sections were placed on an ITO (indium tin oxide) coated glass slide without any adhesive medium (Hudson Surface Technology, Bruker Glass Slides for MALDI imaging [pn 237001], Republic of Korea) and attached to the glass by thaw-mounting. The sections were next placed in a desiccator for 90 min. Air was removed from the chamber using a MEMVAK 2x1 membrane pump to a 30 mbar pressure level at room temperature. A solution of α-cyano-4-hydroxycinnamic acid (Sigma-Aldrich, USA) with a concentration of 5 mg/mL in a 50/50 water/acetonitrile mixture with 0.1% trifluoroacetic acid (TFA, Sigma-Aldrich, USA) was diluted twice. The diluted solution was sprayed using an Iwata Micron CM-B2 airbrush (Anest Iwata, Japan) for 2 sec and allowed to dry for 2.5 min. This process was repeated 20 times.

RNA library and assessing sequencing data

RNA data acquisition, equipment, reagents and processing were done as described in [18]. Briefly, the libraries for sequencing were prepared following an RNA selection protocol utilizing polyadenylation (poly-A selection) and sequenced using the Illumina Hiseq 4000 platform. The raw data were filtered to discard low-quality reads and adapter sequences, then mapped and aligned to human reference genome GRCh38. Data provided in transcripts per million (TPM) was further log-transformed and normalized.

Modules combining functionally similar transcripts were identified using algorithms based on the HumanBase networks [19], which predict gene interactions based on large data sets specific to different types of tissue and regions of the brain covered by more than 14,000 publications. The list of differentially expressed genes in schizophrenia obtained in this work was assessed for the reliability of its correspondence to each of the 144 functions listed in the database. *Corpus callosum* was taken as a reference tissue for the functional analysis. Functional modules were determined by the software based on a community detection algorithm from a provided list of genes and the selected relevant tissue (brain). Genes within a cluster share local network neighborhoods and together form a cohesive, specific functional module.

Lipid extraction

Before lipid extraction, tissue pieces (10–15 mg) were transferred to pre-chilled reinforced 2 ml Precellys tubes (Bertin Technologies). The extraction buffer (MeOH:MTBE, 1:3, v/v) was spiked with the following lipid standards to reach a concentration of 0.5 µg/ml: TAG (15:0/18:1-d7/15:0, Avanti Lipids, 791648C), DAG (15:0/18:1-d7, Avanti Lipids, 791647C), Cer (d18:1-d7/15:0, Avanti Lipids, 860681), LPC (18:1-d7, Avanti Lipids, 791643C), PG (15:0/18:1-d7, Avanti Lipids, 791615C), PC (15:0/18:1-d7, Avanti Lipids, 791637C), PE (15:0/18:1-d7, Avanti Lipids, 791638C). The buffer was prepared once, stored at −20 °C, and was used for all the samples in the batch. Prior to preparation, samples were randomly mixed. "Blank" samples, representing empty tubes without brain tissue, were also processed after biological samples. For lipid extraction, 1 ml of buffer was added to each tube, followed by the homogenization of tissue pieces using the Precellys Evolution homogenizer (Bertin Technologies). Then the samples were shaken on an orbital shaker (30 min, 4 °C) and processed in an ultrasonic bath (10 min, 0 °C). The suspension was then transferred to a new tube (2 ml), and 700 µl of a H_2O:MeOH mixture (3:1, v/v) was added. The resulting mixture was shaken on an orbital shaker (5 min, 4 °C) and centrifuged (11,500 g, 10 min, 4 °C). After centrifugation, 540 µl of the upper phase containing hydrophobic compounds (lipids) was collected, transferred to a 1.5 ml new tube, and the organic solvent was removed using a rotary evaporator

(Thermo Scientific SpeedVac) in ambient temperature. The obtained dry lipid samples were stored at −80 °C.

HPLC-MS analysis

To reconstitute the dry lipid fraction, 200 µl of a pre-cooled (0 °C) mixture of acetonitrile:isopropanol (7:3, v/v) was added to each sample. The samples were shaken on an orbital shaker (10 min, 4 °C), followed by incubation in an ultrasonic bath (10 min, 0 °C), and centrifugation (11,500 g, 10 min, 4 °C). For the preparation of quality control (QC) samples, 5 µl of each sample was pooled. Prior to mass spectrometric analysis, 25 µl of each sample was transferred into 200 µl vials and diluted with an acetonitrile:isopropanol mixture (7:3, v/v) at a ratio of 1:15 for positive polarity and with no dilution for negative polarity measurements. QC samples were introduced at the beginning of the mass spectrometric analysis to condition the column and then after every 12th sample in the series.

The analysis was conducted on a Bruker Impact II Quadrupole Time-of-Flight (QTOF) mass spectrometer (Bruker Daltonics, Bremen, Germany), coupled with the Waters Acquity HPLC chromatographic system (Waters, Manchester, UK) using a method adapted from [20]. Chromatographic separation was performed using a reversed-phase ACQUITY HPLC BEH C8 column (2.1×100 mm, 1.7 µm, Waters Co., Milford, Massachusetts, USA) with a Vanguard pre-column of the same sorbent. The column temperature was maintained at 60 °C. The injection volume was 3 µl. Mobile phase A consisted of 10 mM ammonium acetate in water with 0.1% formic acid, and mobile phase B consisted of 10 mM ammonium acetate in a mixture of acetonitrile:isopropanol (7:3, v/v) with 0.1% formic acid. The flow rate was set to 0.4 ml/min in the following gradient of elution: 1 min — 55% B; 3 min — linear gradient from 55% to 80% B; 8 min — linear gradient from 80% B to 85% B; 3 min — linear gradient from 85% B to 100% B. The phase composition was held at 100% B for 4.5 min, after which the column was re-conditioned at 55% B for 4.5 min. Mass spectrometry detection was performed in full scan mode for positive and negative ions separately within the 50–1,200 m/z range. Source settings in positive polarity were as follows: capillary voltage 4,000 V, nebulizer 2 bar, dry gas 6.0 l/min, and dry temperature 180 °C. MS settings for negative polarity were as follows: capillary voltage 4,000 V, nebulizer 2 bar, dry gas 6.0 l/min, and dry temperature 200 °C. The calibration solution of ammonium formate was infused every injection run.

To assess the lipid molecular structure, we conducted a fragmentation of the pre-selected m/z values. While keeping the chromatographic separation conditions, mass spectra were acquired using a hybrid Q Exactive instrument in the data-dependent (DDA) mode, separately recording spectra in the positive and negative modes. In each mode, the resulting spectra were generated by averaging three fragmentation spectra at different collision energies. A Q Exactive mass spectrometer equipped with a heated electrospray ionization source from Thermo Fisher Scientific (USA) had the following tune parameters: capillary temperature: 320 °C; aux gas heater temperature: 350 °C; capillary voltage: 4.5 kV (−3.5 kV); S-lens RF level: 60; sheath gas flow rate (N2): 45 arbitrary units (a.u.); auxiliary gas flow rate (N2): 20 a.u., sweep gas flow rate (N2): 4 a.u. The operational parameters of the mass spectrometer for the full scan mode were configured as follows: resolution: 70,000 at m/z 200; automatic gain control (AGC target): 5e5; maximum injection time (IT): 50 ms; scan range: 200 to 2,000 Da. For DDA mode: resolution 17,500 at m/z 200; AGC: 2e4; IT: 100 ms; mass isolation window: 1.2 Da; retention time window width: expected time ± 1 min; stepped normalized collision energy: 15%, 25%, 30%; dynamic exclusion: 12 sec; inclusion: on; customize tolerances: 10 ppm. The spectra were recorded in profile mode.

HPLC-MS data processing

Following the acquisition process, the Bruker raw data files (.d files) underwent automatic internal and lock mass calibration before being transformed into the mzXML format using a customized DataAnalysis script from Bruker (Version 4.3). The mzXML files were then imported into the XCMS software using the xcms package within R version 3.8.2. Mass spectrometric peaks falsely duplicated during the XCMS peak merging procedure were identified using a 10 ppm mass threshold within one second retention time difference. Peaks detected during the first minute of the run (retention time <1 min) and after retention time = 18.3 min were excluded from further analysis. The 'fillpeaks' procedure implemented in the xcms package was used for missing value imputation. The lipid intensity values missing after the 'fillpeaks' procedure were filled by random sampling from a normal distribution with the mean equaling the median of minimal intensity values of detected lipid peaks and the standard deviation equaling the 16th percentile of this distribution.

The .raw files were converted to the .abf format using the ABF-converter. Thereafter, the files were processed using the MS-DIAL software (version 4.90) separately for the positive and negative modes. The processing parameters were set as follows: the maximum allowable range for MS1 — 0.05; minimum peak height — 10,000; and mass window width — 0.05. Other parameters were kept at default values and remained unchanged. An internal lipid database was employed for lipid annotation, encompassing 34 lipid classes based on previous brain studies (PC, PC-O, PE, PE-O, PE-P, PS, PA, PG, BMP, PI, LPC, LPE, LPC-O, LPE-O, LPS, LPA, LPG, AHexCer, Cer, HexCer, SHexCer, SM, ST, CE, TAG, DAG, MAG, MGDG, DGDG, MGDG-O, DGDG-O, FFA, CAR, NAE). The obtained databases of lipid compound areas were exported and processed in the R environment. Polarities were merged, and lipid duplicates between the two polarities were filtered based on retention time overlap and exact mass. Annotations obtained with the Q Exactive instrument were aligned with peaks in a QTOF analysis based on the retention time and m/z ratio.

To ensure a high quality of the annotated peaks, account for the extraction chemical noise and technical variability, filtering procedures were applied on the resulting target list. Firstly, a blank samples filter was applied: only those features with a mean intensity at least twice greater than in the blanks were selected for further analysis. Secondly, a variance filter was applied: the coefficient of variation was calculated across QC samples for each peak, and only those peaks with a median coefficient of variation (CV) below 0.25 were selected.

After that, all lipid intensities were log10-transformed and normalized on the median value of standards within a sample and wet weight of the sample. For normalization purposes, wet weights and standard intensities were log10-transformed, then the difference of sample values from the mean of a parameter was subtracted. Resulting lipid intensity values were further normalized using the mean intensity of the lipid calculated within each individual's brain to adjust for inter-individual variability.

MALDI experiment

MALDI-MSI data acquisition, equipment, reagents, peak annotation, and processing were done as described in [21]. Briefly, MALDI images were obtained using a modified Thermo Scientific Q Exactive Orbitrap mass spectrometer equipped with a 355 nm Nd:YAG laser. Imaging involved controlling the tissue region and raster step size with the Spectroglyph software and collecting spectra at 40-µm intervals in both dimensions. Ion images were generated from raw and coordinate files using the Image Insight software. The raw mass spectra were converted to the .ibd and .imzML formats with a zero background noise threshold, and further processing was conducted using Cardinal 2.8.0, an R package for mass spectrometry imaging data analysis. For image analysis, duplicate coordinates were removed and peak intensities were normalized by total ion current. Peak picking was performed using a signal-to-noise ratio threshold of three. Spectra were aligned to the average spectrum, and the peaks that were present in less than 7% of the spectra were excluded.

Peaks from the glass slide surface and uninformative spectrum parts were removed. The sample area was divided using a spatial k-means algorithm to distinguish between tissue and sample-free areas. Clusters were manually curated, and only peaks with 1.5 times greater mean intensities in the tissue cluster were retained. Finally, all the spectra were aligned to the one with the most detected peaks.

The peaks were annotated as lipid species based on their mass-to-charge ratio, with the mass difference threshold between the data and target values set to 20 ppm. For cases of multiple matches, the rules described in [21] were applied.

Statistical analysis

Lipid intensities were log10-transformed, and the average across all individuals in a group was used for further analysis. Next, differences between the peak averages of the two groups were calculated and the one-sample Student t-test was applied to test whether the resulting distribution of mean peak intensities differed significantly from zero. The Benjamini-Hochberg correction for multiple hypothesis testing was used. Data analysis and visualization were performed using R packages (Ggplot2, MixOmics, and other standard R packages).

To compare our dataset with previously published data on lipidomic alterations in the SZ-affected corpus callosum [7], log2 transformation was applied to downloaded original fold changes in lipid intensities. Lipid compounds were matched manually based on annotation (HPLC-MS data) or exact mass (MALDI) with respect to the common adducts. To compare with MALDI data, all detected m/z values were rounded to two decimal and only lipids that exactly matched by mass were used in the analysis. To compare HPLC-MS

data, mean fold changes were calculated for each class. Only lipid classes containing more than three lipids were used in the analysis. Pearson's correlation coefficient was then calculated based on the log2 fold changes of lipid compounds matched between datasets.

Differences in the distribution of lipids across the corpus callosum sections were assessed via the coefficient of variance (CoV). The coefficient for the control and schizophrenia groups was calculated for the masses annotated by HPLC-MS as the ratio of the standard deviation to the mean for each mass. The difference in the CoV for the two groups was tested using the Wilcoxon signed-rank test.

Ethical approval

The data for the brain samples obtained from National BioService contained no personal information or any other information that could allow donors identification. Informed consent for the use of the biomaterial for research purposes were secured from the individuals or from the next-of-kin at the respective clinical organizations that provided the samples to National BioService in accordance with international regulations[2].

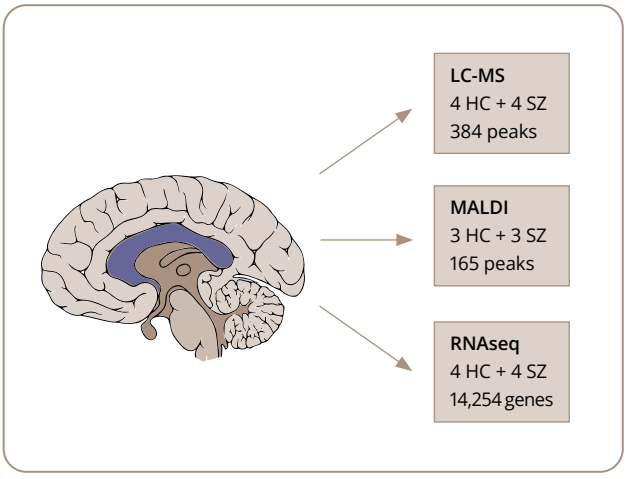

Figure 1. Experiment design.

Note: Samples of corpus callosum were dissected and used for three types of measurements: HPLC-MS; MALDI-MSI and RNAseq. Number of features detected in each type of analysis provided on the plot. HC — healthy controls; HPLC-MC — high-performance liquid chromatography with mass spectrometry; MALDI-MSI — matrix-assisted laser desorption/ionization mass spectrometric imaging; RNAseq — sequencing of ribonucleic acid; SZ — schizophrenia patients.

Source: Osetrova et al., 2025.

RESULTS

We examined the alterations in the white matter lipidome composition between SZ and HC individuals using HPLC-MS, as well as MALDI-MSI (Table S1 in the Supplementary).

The application of each technique resulted in the detection of 384 and 165 lipid features for HPLC-MS and MALDI, respectively (Figure 1; Tables S2 and S3 in the Supplementary). Additionally, we measured changes in the RNA expression in the brain region associated with schizophrenia, which resulted in the evaluation of 14,254 genes expressed in the corpus callosum (Figure 1).

For each of the 20 lipid classes detected with HPLC-MS, we calculated mean intensities for the SZ and HC groups and conducted the one-sample Student t-test of the differences between groups vs zero to evaluate the class-level differences characteristic of schizophrenia (Figure 2A). For two lipid classes, such as diacylglycerols (DG) and free fatty acids (FA), significant upregulation was detected in schizophrenia samples. In contrast, the majority of lipid classes (seven classes) demonstrated significantly lower levels in SZ samples compared to the HC. Among them are phosphatidylcholines (PC) and phosphatidylethanolamines (PE) — the major components of cell membranes; three classes previously shown to be components of the myelin sheath — sphingomyelins (SM), hexosylceramides (HexCer), and sulfohexosylceramides (SulfoHexCer); triacylglycerides (TG) used as lipid storage substrate; and phosphatidylglycerols (PG), which are synthesized in mitochondria (Figure 2A). The demonstrated differences in the level of lipid classes are in good agreement with previously reported lipidome alterations data in a corpus callosum associated with schizophrenia [7], with Pearson's R=0.74 (p=0.0142), calculated based on the same 10 lipid classes measured in two works (Figure 2B).

MALDI imaging yielded similar results with a statistically significant lower average peak intensity evaluated via one-sample Student t-test for the distribution of the differences between peaks averages between the two groups for all peaks (p=0.0013) (Figure 2C). Additionally, the coefficient of variance across all MALDI pixels calculated for each peak intensity differed significantly between the schizophrenia and control groups (Wilcoxon signed-rank test, p <4e-10, Figure 2D). For a subset of peaks matched with the HPLC-MS result, good agreement was demonstrated between the two mass spectrometric techniques with R=0.77 and p=0.0061

[2] National BioService, LLC.

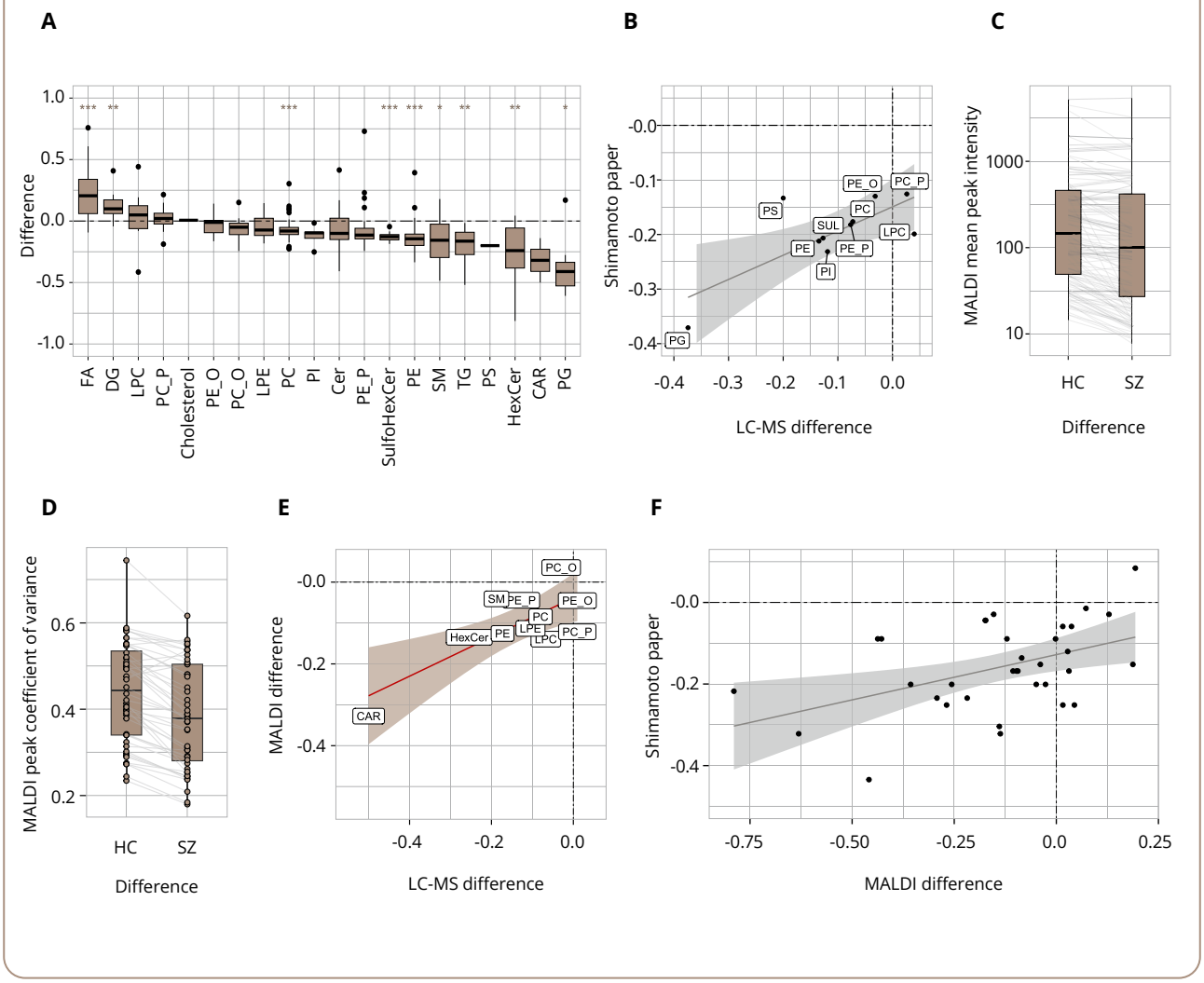

Figure 2. Schizophrenia-associated lipidome alterations in corpus callosum between the groups of patients with schizophrenia and the group of healthy controls.

Note: (A) Boxplots representing differences in lipid intensities between SZ patients and the HC for each lipid class, measured with HPLC-MS. Asterisks reflect the statistical significance of the difference evaluated via a one-sample Student t-test of the differences between groups vs zero for each class (*** — p <0.001; ** — p <0.01; * — p <0.05; p-values corrected for multiple hypothesis testing). Positive values represent higher levels in the schizophrenia group. (B) Correlation of average differences for each lipid class correlated to the published paper on the corpus callosum lipidome in schizophrenia by Shimamoto et al. [7]. The correlation is calculated based on the same 10 lipid classes measured in two works. (C) Boxplots of the peak intensity distribution for the MALDI imaging experiment. Each line connects the same peak in two sample groups. One-sample Student t-test was used to determine whether the distribution of the differences between peak averages between the two groups differed statistically significantly from zero (p=0.0013). (D) Boxplots of the coefficient of variance calculated for each MALDI peak within each group. Statistical significance of the differences between the coefficients of variance evaluated via the Wilcoxon signed-rank test (p <4e-10). Lines connect the same lipid intensity averaged within different groups. (E) Correlation of average differences for each lipid class between the two types of measurements (HPLC-MS and MALDI-MSI). (F) Correlation with [7] for the MALDI imaging experiment. Peaks-plotting was based on mass-matching, and one dot represents one matched peak.

Linear regression lines on the plots B, E, and F are drawn with CI=95% by shaded areas, demonstrating that all the represented correlations are statistically significant and positive. Full names for the lipid classes present in the Box 1 in the Supplementary. The box boundaries in the boxplots represent the 25% and 75% percentiles, the lines represent the spread, and statistical outliers are indicated by dots.

HC — healthy controls; HPLC-MC — high-performance liquid chromatography with mass spectrometry; MALDI-MSI — matrix-assisted laser desorption/ionization mass spectrometric imaging; SZ — schizophrenia patients.

Source: Osetrova et al., 2025.

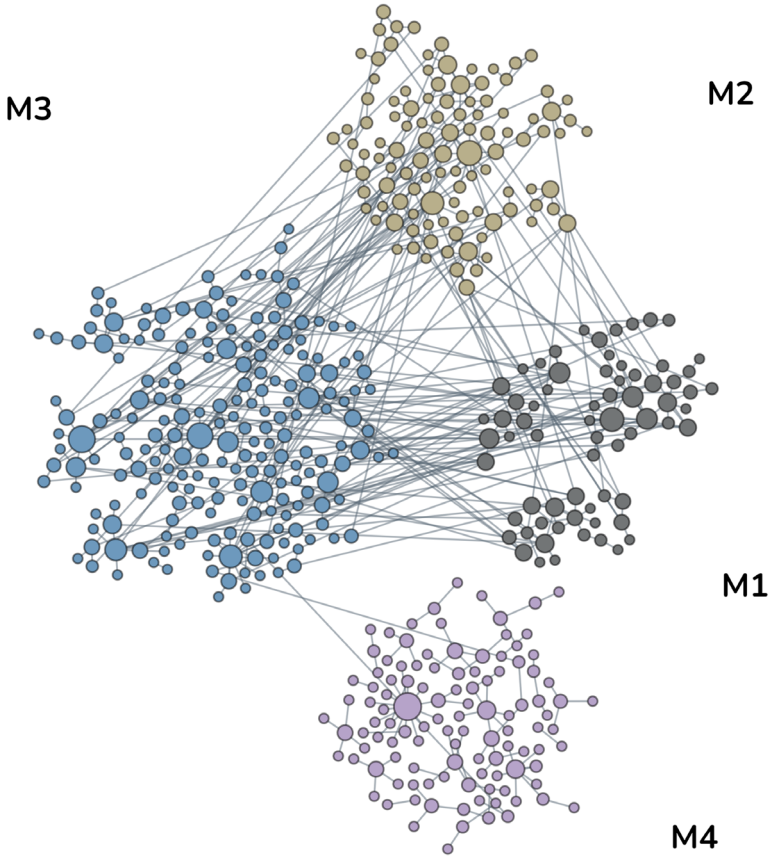

Module	Top terms (Max 10)	Genes	Terms
M1	Cytoplasmic translation; translation; peptide biosynthetic process; amide biosynthetic process; peptide metabolic process; ribonucleoprotein complex biogenesis; ribosome biogenesis; regulation of translation; erythrocyte differentiation; regulation of cellular amide metabolic process.	69	54
M2	Negative regulation of extrinsic apoptotic signaling pathway via death domain receptors; regulation of extrinsic apoptotic signaling pathway via death domain receptors; regulation of extrinsic apoptotic signaling pathway; extrinsic apoptotic signaling pathway via death domain receptors; negative regulation of extrinsic apoptotic signaling pathway; histone acetylation; internal peptidyl-lysine acetylation; internal protein amino acid acetylation; peptidyl-lysine acetylation; spindle organization.	108	75
M3	Epithelial cell migration; tissue migration; epithelium migration; ameboidal-type cell migration; regulation of cell morphogenesis; regulation of cell shape; endothelial cell migration; cellular component morphogenesis; cell morphogenesis; regulation of epithelial cell migration.	203	120
M4	Fatty acid biosynthetic process; monocarboxylic acid biosynthetic process; chloride transmembrane transport; small molecule biosynthetic process; photoreceptor cell maintenance; chloride transport; response to fatty acid; inorganic anion transmembrane transport; unsaturated fatty acid biosynthetic process; retina homeostasis.	112	39

Figure 3. Modules of genes in the corpus callosum with differential expression between the group of patients with schizophrenia and the group of healthy controls.

Note: One dot represents one gene, colored according to module assignment, edges represent functional association between two genes, the size of the dots reflects the number of edges. The five most statistically significant functional terms for each module are presented in the Table S5 in the Supplementary.

Source: Osetrova et al., 2025.

(Figure 2E). If calculated without the most outstanding class, the carnitines, the correlation remained positive, but not statistically significant (R=0.29; p=0.42). Finally, MALDI peaks matched with Shimamoto et al. [7] demonstrated a statistically significant positive correlation between two datasets with R=0.46 and p=0.0066 (Figure 2F).

The analysis of 14,254 transcripts in specimens of the corpus callosum revealed 1,202 (8.4%) differentially expressed genes between the groups of patients with SZ and HC (Table S4 in the Supplementary). Twenty genes out of the 1,202 were excluded from the analysis due to the lack of information about them in the HumanBase. As a result, four functional modules were identified, which included 492 of the detected genes (Figure 3, Table S5 in the Supplementary). The main cellular functions of the M1 module are the following: cytoplasmic translation, translation, peptide biosynthetic process, amide biosynthetic process, and peptide metabolic process; module M2: negative regulation of extrinsic apoptotic signaling pathway via death domain receptors, regulation of extrinsic apoptotic signaling pathway via death domain receptors, regulation of extrinsic apoptotic signaling pathway, extrinsic apoptotic signaling pathway via death domain receptors, and negative regulation of the extrinsic apoptotic signaling pathway; module M3: epithelial cell migration, tissue migration, epithelium migration, ameboidal-type cell migration, and regulation of cell morphogenesis; module M4: fatty acid biosynthetic process, monocarboxylic acid biosynthetic process, chloride transmembrane transport, small molecule biosynthetic process, and photoreceptor cell maintenance.

DISCUSSION

Key results

The analysis of the alterations in the lipid composition of the corpus callosum of the brain of patients with schizophrenia using two mass spectrometric methods demonstrated a trend towards overall lower lipid levels for the most observed classes and consistency between techniques and studies. Among lipid classes with the most noticeable discrepancies are the ones previously associated with myelin sheath formation. Analysis of spatial-dispersion-of-lipids-across-the-corpus-callosum slides revealed a more homogeneous distribution for samples taken from schizophrenia patients. Functional gene analysis also identified a module associated with lipid metabolism.

Limitations

One of the major limitations of our study is the limited sample size, especially taking into account the high heterogeneity of the disease. Moreover, our study design did not exclude the potential influence of confounding variables, such as the use of antipsychotic medication, on the lipid composition of the white matter tracts of the brain. However, despite this, we observed a statistically significant correlation between two independent mass spectrometry experiments on different subsamples, as well as a correlation with previously published data obtained from a larger sample of individuals. Moreover, even with the possible "noise" of individual lipid measurements and annotation, the results at the lipid class level are consistent and reproducible. Another limitation of the article concerns the statistical analysis. Using unpaired comparison methods for the difference in the mean lipid levels and their CoV between groups, statistically significant differences were not observed (p >0.05 for the two-sample Student's t-test and the Mann-Whitney test, respectively). On the one hand, this may be due to the small effect size. On the other hand, the reason might be the fact that different lipids have a large spread of characteristic values due to methodological limitations, which makes the variance within sample groups comparable to the total variance for both groups.

Interpretation

Although previous studies had detected a few [7] or no [22] statistically significant differences between schizophrenia patients and control groups, we demonstrated class-level consistency in the direction of the differences, both for different techniques and in comparison of our results to previously published data on the subset of classes in intersection. Free fatty acids showed the greatest difference towards the higher level, which is also consistent in the direction of differences with the results of previous work from our group [23] and may be a general marker of lipid metabolism disorders characteristic of schizophrenia. Importantly, corpus callosum was the region with the most significant differences, as compared to the other five regions of white matter investigated, although differences at the level of individual classes could diverge, which may be a limitation in the use of a relatively small sample in our study. The decline in the level of lipids associated with myelin sheath formation, such as sulfohexosylceramides sphingomyelins, and hexosylceramides, aligns our results with previously shown disturbances in the myelin structure

detected in schizophrenia using various MRI techniques [24–27]. The decrease in the levels of phosphatidylglycerols might reflect mitochondrial dysfunction, which has also been linked to schizophrenia [23]. Interestingly, elevated levels of triacylglycerides have been designated as biomarkers of schizophrenia with elevated levels in the blood [28, 29]. Differences in the distribution of lipids across the corpus callosum sections assessed via the coefficient of variance for each peak demonstrated a more even intensity distribution for the schizophrenia samples, suggesting a less structured organization of lipids [30]. Such results might be a reflection of disturbances in cellular organization, such as less dense myelin packing and less compartmentalization [31].

The functional gene analysis results align well with recent studies on the disruption of ribosome action in schizophrenia [32, 33], the role of the extrinsic apoptotic pathway in the mechanisms of neuroprotection, the homeostasis of inflammatory reactions and neurodegeneration [34], the influence of alterations in histone acetylation on neuronal migration in schizophrenia [35], the direct connection between the expression of the factors that direct axon growth and the development of interhemispheric commissures [36], the regulation of the balance of excitation/inhibition in the brain by transmembrane transport of chlorides in schizophrenia [37, 38], and the key role of polyunsaturated fatty acids in the inflammatory response of different types of brain cells and dysfunction in neurotransmitter systems [39–42]. In the scope of the current paper, the latter is of special interest as further investigation of genes associated with M4 might help gain a deeper understanding of the discovered lipidome differences in the corpus callosum associated with schizophrenia.

CONCLUSION

We suggest that investigation of the molecular alterations in the composition of the white matter in schizophrenia and the combination of various measuring techniques might help us achieve a deeper understanding of the disease. The application of mass spectrometric neuroimaging methods to the analysis of the white matter composition showed to be a promising technique, with further potential to help peer deeper into the spatial nuances of lipidome alterations.

Article history

Submitted: 13 Dec 2023
Accepted: 27 Feb 2025
Published Online: 17 Mar 2025

Authors' contribution: Conceptualization — Maria Osetrova and Philipp Khaitovich; methodology — Olga Efimova, Gleb Vladimirov and Elena Stekolschikova; software — Maria Osetrova; validation — Maria Osetrova; formal analysis — Maria Osetrova; investigation — Maria Osetrova, Dmitry Senko; resources — Olga Efimova, Tatiana Zhuravleva, Gleb Vladimirov, George Kostyuk and Evgeniy Nikolaev; data curation — Maria Osetrova and Elena Stekolschikova; writing original draft preparation — Maria Osetrova and Marina Zavolskova; writing review and editing — Denis Andreyuk, Yana Zorkina, Anna Morozova and Philipp Khaitovich; visualization — Maria Osetrova; supervision — Philipp Khaitovich; project administration — Philipp Khaitovich. All authors checked and approved final version of the manuscript prior to publication.

Funding: The work of Maria Osetrova was funded by the Russian Science Foundation under grant No. 20-15-00299. The work of Dmitry Senko, Marina Zavolskova, and Olga Efimova was funded by the Russian Science Foundation under grant No. 22-15-00474.

Conflict of interest: The authors declare no conflicts of interest.

Supplementary data

Supplementary material to this article can be found in the online version:
Box 1: https://doi.org/10.17816/CP15491-145517
Table S1: https://doi.org/10.17816/CP15491-145515
Table S2: https://doi.org/10.17816/CP15491-145518
Table S3: https://doi.org/10.17816/CP15491-145519
Table S4: https://doi.org/10.17816/CP15491-145520
Table S5: https://doi.org/10.17816/CP15491-145516

For citation:

Osetrova MS, Efimova OI, Zavolskova MD, Stekolschikova EA, Vladimirov GN, Senko DA, Zhuravleva TA, Morozova AYu, Zorkina YA, Andreyuk DS, Kostyuk GP, Nikolaev EN, Khaitovich PhE. Comparative Analysis of Corpus Callosum Lipidome and Transcriptome in Schizophrenia and Healthy Brain. *Consortium PSYCHIATRICUM.* 2025;6(1):CP15491 doi: 10.17816/CP15491

Information about the authors

***Maria Stanislavovna Osetrova**, Engineer Researcher, V. Zelman Center for Neurobiology and Brain Restoration, Skolkovo Institute of Science and Technology; e-Library SPIN-code: 5813-1688,

Scopus Author ID: 57505703600, ResearcherID: HOH-3453-2023,
ORCID: https://orcid.org/0000-0002-8174-9544
E-mail: maria.osetrova.sk@gmail.com
Olga Igorevna Efimova, Junior Researcher, V. Zelman Center for Neurobiology and Brain Restoration, Skolkovo Institute of Science and Technology; e-Library SPIN-code: 3427-8085,
Scopus Author ID: 15836570500,
ORCID: https://orcid.org/0000-0003-0842-3203
Marina Dmitrievna Zavolskova, Junior Researcher, V. Zelman Center for Neurobiology and Brain Restoration, Skolkovo Institute of Science and Technology; e-Library SPIN-code: 1800-6986,
Scopus Author ID: 57209106743,
ORCID: https://orcid.org/0000-0003-4532-0721
Elena Alekseevna Stekolschikova, Cand. Sci (Chem.), Senior Researcher, V. Zelman Center for Neurobiology and Brain Restoration, Skolkovo Institute of Science and Technology; e-Library SPIN-code: 3859-4534,
Scopus Author ID: 56462907300, ResearcherID: U-1735-2018,
ORCID: https://orcid.org/0000-0001-8607-9773
Gleb Nikolaevich Vladimirov, Cand. Sci (Phys. and Math.), Senior Researcher, V. Zelman Center for Neurobiology and Brain Restoration, Skolkovo Institute of Science and Technology;
Scopus Author ID: 55579659300,
ORCID: https://orcid.org/0000-0003-4623-4884
Dmitry Andreevich Senko, PhD student, V. Zelman Center for Neurobiology and Brain Restoration, Skolkovo Institute of Science and Technology, ORCID: https://orcid.org/0000-0001-8752-9932
Tatiana Alekseevna Zhuravleva, student, Faculty of Fundamental Medicine, Lomonosov Moscow State University
Anna Yurievna Morozova, MD, Cand. Sci (Med.), Senior Researcher, Mental-health clinic No. 1 named after N.A. Alexeev; V. Serbsky National Medical Research Centre of Psychiatry and Narcology of the Ministry of Health of the Russian Federation; e-Library SPIN-code: 3233-7638, ResearcherID: T-1361-2019, Scopus Author ID: 55648593900,
ORCID: https://orcid.org/0000-0002-8681-5299
Yana Alexandrovna Zorkina, Cand. Sci (Biolog.), Senior Researcher, Mental-health clinic No. 1 named after N.A. Alexeev; V. Serbsky National Medical Research Centre of Psychiatry and Narcology of the Ministry of Health of the Russian Federation;
e-Library SPIN-code: 3017-3328, ResearcherID: H-2424-2013,
Scopus Author ID: 54584719100,
ORCID: https://orcid.org/0000-0003-0247-2717
Denis Sergeevich Andreyuk, Cand. Sci (Biolog.), Mental-health clinic No. 1 named after N.A. Alexeev; ResearcherID: AAQ-6260-2020, Scopus Author ID: 6602608643, ORCID: https://orcid.org/0000-0002-3349-5391
George Petrovich Kostyuk, MD, Dr. Sci (Med.), Professor, Head of Mental-health clinic No. 1 named after N.A. Alexeev; Head of the Department of Mental Health and Clinical Psychiatry, Faculty of Psychology, Lomonosov Moscow State University;
e-Library SPIN-code: 3424-4544, ResearcherID: AAA-1682-2020,
Scopus Author ID: 57200081884,
ORCID: https://orcid.org/0000-0002-3073-6305
Evgeniy Nikolaevich Nikolaev, Cand. Sci (Biolog.), Professor, Head of the Mass Spectrometry Laboratory, Center for Molecular and Cellular Biology, Skolkovo Institute of Science and Technology;
e-Library SPIN-code: 4984-1007, Scopus Author ID: 55394217800,
ORCID: https://orcid.org/0000-0001-6209-2068
Philipp Efimovich Khaitovich, Cand. Sci (Biolog.), Professor, Director of the V. Zelman Center for Neurobiology and Brain Restoration, Skolkovo Institute of Science and Technology; Scopus Author ID: 6602559039,
ORCID: https://orcid.org/0000-0002-4305-0054

*corresponding author

References

1. Wang D, Sun X, Maziade M, et al. Characterising phospholipids and free fatty acids in patients with schizophrenia: A case-control study. World J Biol Psychiatry. 2021;22(3):161–174. doi: 10.1080/15622975.2020.1769188
2. Schmitt A, Wilczek K, Blennow K, et al. Altered thalamic membrane phospholipids in schizophrenia: a postmortem study. Biol Psychiatry. 2004;56(1):41–45. doi: 10.1016/j.biopsych.2004.03.019
3. Miyahara K, Hino M, Shishido, et al. Identification of schizophrenia symptom-related gene modules by postmortem brain transcriptome analysis. Transl Psychiatry. 2023;13(1):144. doi: 10.1038/s41398-023-02449-8
4. Türk Y, Ercan I, Sahin I, et al. Corpus callosum in schizophrenia with deficit and non-deficit syndrome: a statistical shape analysis. Gen Psychiatr. 2021;34(6):e100635. doi: 10.1136/gpsych-2021-100635
5. Wang P, Jiang Y, Hoptman MJ, et al. Structural–functional connectivity deficits of callosal–white matter–cortical circuits in schizophrenia. Psychiatry Res. 2023;330:115559. doi: 10.1016/j.psychres.2023
6. Yoon JH, Seo Y, Jo YS, et al. Brain lipidomics: From functional landscape to clinical significance. Sci Adv. 2022;8(37):eadc9317. doi: 0.1126/sciadv.adc9317
7. Shimamoto-Mitsuyama C, Nakaya A, Esaki K, et al. Lipid Pathology of the Corpus Callosum in Schizophrenia and the Potential Role of Abnormal Gene Regulatory Networks with Reduced Microglial Marker Expression. Cereb Cortex. 2021;31(1):448–462. doi: 10.1093/cercor/bhaa236
8. Esaki K, Balan S, Iwayama Y, et al. Evidence for Altered Metabolism of Sphingosine-1-Phosphate in the Corpus Callosum of Patients with Schizophrenia. Schizophr Bull. 2020;46(5):1172–1181. doi: 10.1093/schbul/sbaa052
9. Zhao X, Zhang S, Sanders AR, et al. Brain Lipids and Lipid Droplet Dysregulation in Alzheimer's Disease and Neuropsychiatric Disorders. Complex Psychiatry. 2023;9(1-4):154–171. doi: 10.1159/000535131
10. Xu K, Zheng P, Zhao S, et al. Altered MANF and RYR2 concentrations associated with hypolipidemia in the serum of patients with schizophrenia. J Psychiatr Res. 2023;163:142–149. doi: 10.1016/j.jpsychires.2023.05.044
11. Fizíková I, Dragašek J, Račay P. Mitochondrial Dysfunction, Altered Mitochondrial Oxygen, and Energy Metabolism Associated with the Pathogenesis of Schizophrenia. Int J Mol Sci. 2023;24(9). doi: 10.3390/ijms24097991
12. Ghosh S, Dyer RA, Beasley CL. Evidence for altered cell membrane lipid composition in postmortem prefrontal white matter in bipolar disorder and schizophrenia. J Psychiatr Res. 2023;95:135–142. doi: 10.1016/j.jpsychires.2017.08.009
13. Howes OD, Onwordi EC. The synaptic hypothesis of schizophrenia version III: a master mechanism. Mol Psychiatry. 2023;28(5):1843–1856. doi: 10.1038/s41380-023-02043-w
14. Hussain G, Anwar H, Rasul A, et al. Lipids as biomarkers of brain disorders. Crit Rev Food Sci Nutr. 2020;60(3):351–374. doi: 10.1080/10408398.2018.1529653
15. Perez JM, Berto S, Gleason K, et al. Hippocampal subfield transcriptome analysis in schizophrenia psychosis. Mol Psychiatry. 2021;26(6):2577–2589. doi: 10.1038/s41380-020-0696-6
16. Lindholm Carlström E, Niazi A, Etemadikhah, et al. Transcriptome Analysis of Post-Mortem Brain Tissue Reveals Up-Regulation of the Complement Cascade in a Subgroup of Schizophrenia Patients. Genes (Basel). 2021;12(8). doi: 10.3390/genes12081242

17. Mai JK, Majtanik M, Paxinos G. Atlas of the Human Brain. Cambridge: Academic Press; 2015.
18. Khrameeva E, Kurochkin I, Han D, et al. Single-cell-resolution transcriptome map of human, chimpanzee, bonobo, and macaque brains. Genome Res. 2020;30(5):776–789. doi: 10.1101/gr.256958.119
19. Greene CS, Krishnan A, Wong AK, et al. Understanding multicellular function and disease with human tissue-specific networks. Nat Genet. 2015;47(6):569–576. doi: 10.1038/ng.3259
20. Senko D, Gorovaya A, Stekolshchikova E, et al. Time-Dependent Effect of Sciatic Nerve Injury on Rat Plasma Lipidome. Int J Mol Sci. 2022;23(24):15544. doi: 10.3390/ijms232415544
21. Osetrova M, Zavolskova M, Mazin P, et al. Mass spectrometry imaging of two neocortical areas reveals the histological selectivity of schizophrenia-associated lipid alterations. Consort Psychiatr. 2024;5(3):4–16. doi: 10.17816/CP15488
22. Hamazaki K, Maekawa M, Toyota T, et al. Fatty acid composition of the postmortem corpus callosum of patients with schizophrenia, bipolar disorder, or major depressive disorder. Eur Psychiatry. 2017;39:51–56. doi: 10.1016/j.eurpsy.2016.05.007
23. Senko D, Efimova O, Osetrova M, et al. White matter lipidome alterations in the schizophrenia brain. Schizophrenia (Heidelb). 2024;10(1):123. doi: 10.1038/s41537-024-00542-5
24. Kelly S, Jahanshad N, Zalesky A, et al. Widespread white matter microstructural differences in schizophrenia across 4322 individuals: results from the ENIGMA Schizophrenia DTI Working Group. Mol Psychiatry. 2018;23(5):1261–1269. doi: 10.1038/mp.2017.170
25. Smirnova LP, Yarnykh VL, Parshukova DA, et al. Global hypomyelination of the brain white and gray matter in schizophrenia: quantitative imaging using macromolecular proton fraction. Transl Psychiatry. 2021;11(1):365. doi: 10.1038/s41398-021-01475-8
26. Iwatani J, Ishida T, Donishi T, et al. Use of T1-weighted/T2-weighted magnetic resonance ratio images to elucidate changes in the schizophrenic brain. Brain Behav. 2015;5(10):e00399. doi: 10.1002/brb3.399
27. Carreira Figueiredo I, Borgan F, Pasternak O, et al. White-matter free-water diffusion MRI in schizophrenia: a systematic review and meta-analysis. Neuropsychopharmacology. 2022;47(7):1413–1420. doi: 10.1038/s41386-022-01272-x
28. Tkachev A, Stekolshchikova E, Vanyushkina A, et al. Lipid Alteration Signature in the Blood Plasma of Individuals With Schizophrenia, Depression, and Bipolar Disorder. JAMA Psychiatry. 2023;80(3):250–259. doi: 10.1001/jamapsychiatry.2022.4350
29. Solberg DK, Bentsen H, Refsum H, et al. Lipid profiles in schizophrenia associated with clinical traits: a five year follow-up study. BMC Psychiatry. 2016;16(1):299. doi: 10.1186/s12888-016-1006-3
30. Valdés-Tovar M, Rodríguez-Ramírez AM, Rodríguez-Cárdenas L, et al. Insights into myelin dysfunction in schizophrenia and bipolar disorder. World J Psychiatry. 2022;12(2):264–285. doi: 10.5498/wjp.v12.i2.264
31. Davis KL, Stewart DG, Friedman JI, et al. White matter changes in schizophrenia: evidence for myelin-related dysfunction. Arch Gen Psychiatry. 2003;60(5):443–456. doi: 10.1001/archpsyc.60.5.443
32. Liang Q, Jiang Y, Shieh AW, et al. The impact of common variants on gene expression in the human brain: from RNA to protein to schizophrenia risk. bioRxiv [Preprint]. 2023:2023.06.04.54363. doi: 10.1101/2023.06.04.543603
33. Mekiten O, Yitzhaky A, Gould N, et al. Ribosome subunits are upregulated in brain samples of a subgroup of individuals with schizophrenia: A systematic gene expression meta-analysis. J Psychiatr Res. 2023;164:372–381. doi: 10.1016/j.jpsychires.2023.06.013
34. Vitale I, Pietrocola F, Guilbaud E, et al. Apoptotic cell death in disease-Current understanding of the NCCD 2023. Cell Death Differ. 2023;30(5):1097–1154. doi: 10.1038/s41418-023-01153-w
35. Borrie SC, Bagni C. Neurons acetylate their way to migration. EMBO Rep. 2016;17(12):1674–1676. doi: 10.15252/embr.201643427
36. Tsuji Y, Kerever A, Furukawa T, et al. Diffusion magnetic resonance tractography-based evaluation of commissural fiber abnormalities in a heparan sulfate endosulfatase-deficient mouse brain. Magn Reson Imaging. 2022;88:123–131. doi: 10.1016/j.mri.2022.01.017
37. Lam P, Newland J, Faull RLM, et al. Cation-Chloride Cotransporters KCC2 and NKCC1 as Therapeutic Targets in Neurological and Neuropsychiatric Disorders. Molecules. 2023;28(3):1344. doi: 10.3390/molecules28031344
38. Hui KK, Chater TE, Goda Y, et al. How Staying Negative Is Good for the (Adult) Brain: Maintaining Chloride Homeostasis and the GABA-Shift in Neurological Disorders. Front Mol Neurosci. 2022;15:893111. doi: 10.3389/fnmol.2022.893111
39. Zhang Y, Yin J, Yan H, et al. Correlations between omega-3 fatty acids and inflammatory/glial abnormalities: the involvement of the membrane and neurotransmitter dysfunction in schizophrenia. Front Cell Neurosci. 2023;17:1163764. doi: 10.3389/fncel.2023.1163764
40. Gao Y, Hu X, Wang D, et al. Association between Arachidonic Acid and the Risk of Schizophrenia: A Cross-National Study and Mendelian Randomization Analysis. 2023;15(5):1195. doi: 10.3390/nu15051195
41. Le ATP, Higuchi Y, Sumiyoshi T, et al. Analysis of polyunsaturated fatty acids in antipsychotic-free individuals with at-risk mental state and patients with first-episode schizophrenia. Front Psychiatry. 2023;14:1188452. doi: 10.3389/fpsyt.2023.1188452
42. Yamamoto Y, Owada Y. Possible involvement of fatty acid binding proteins in psychiatric disorders. Anat Sci Int. 2021;96(3):333–342. doi: 10.1007/s12565-020-00598-0